Journal of Medical Systems (2019) 43: 118
https://doi.org/10.1007/s10916-019-1245-1

IMAGE & SIGNAL PROCESSING

A Novel Distributed Multitask Fuzzy Clustering Algorithm for Automatic MR Brain Image Segmentation

Yizhang Jiang [1] · Kaifa Zhao [1] · Kaijian Xia [2] · Jing Xue [3] · Leyuan Zhou [4] · Yang Ding [4] · Pengjiang Qian [1]

Received: 26 November 2018 / Accepted: 14 March 2019 / Published online: 25 March 2019

Abstract

Artificial intelligence algorithms have been used in a wide range of applications in clinical aided diagnosis, such as automatic MR image segmentation and seizure EEG signal analyses. In recent years, many machine learning-based automatic MR brain image segmentation methods have been proposed as auxiliary methods of medical image analysis in clinical treatment. Nevertheless, many problems regarding precise medical images, which cannot be effectively utilized to improve partition performance, remain to be solved. Due to the poor contrast in grayscale images, the ambiguity and complexity of MR images, and individual variability, the performance of classic algorithms in medical image segmentation still needs improvement. In this paper, we introduce a distributed multitask fuzzy c-means (MT-FCM) clustering algorithm for MR brain image segmentation that can extract knowledge common among different clustering tasks. The proposed distributed MT-FCM algorithm can effectively exploit information common among different but related MR brain image segmentation tasks and can avoid the negative effects caused by noisy data that exist in some MR images. Experimental results on clinical MR brain images demonstrate that the distributed MT-FCM method demonstrates more desirable performance than the classic signal task method.

Keywords MR brain image · Distributed multitask fuzzy clustering · Medical image · Image segmentation

Introduction

In recent years, the development of medical imaging technologies, such as computed tomography (CT) scanning, positron emission tomography (PET) scanning, and magnetic resonance imaging (MRI), have revolutionized diagnostics. Modern clinical diagnosis tends to have the advantages of accuracy, precision, dynamism, microquantization, automation and noninvasiveness. Medical imaging technologies, which provide images of the anatomy structure of the human body, have become important in modern clinical diagnosis. Currently, many artificial intelligence technologies have been applied to medical image processes, such as MR image segmentation, lesion area extraction, and 3D reconstruction, to assist doctors in qualitatively and quantitatively analyzing lesions and specific areas and in facilitating the development of medical diagnoses.

Multimodal medical imaging technologies, such as PET/MR and PET/CT, have been proposed to improve the quality of medical images and to overcome some disadvantages of existing medical images. Many MR sequences can be achieved by one-time scanning, such as free induction decay (FID), the Dixon method, and $R2^*$. Among these sequences, ultrashort echo time (UTE) imaging can effectively extract bone from air, and the Dixon-based approach can divide soft tissue into fat and water components [1–3]. In addition, these multimodal images could also facilitate the understanding of brain diseases and disorders such as Alzheimer's disease, Parkinson's disease, and autism. Since only limited knowledge can be exploited from a single subject's medical image,

This article is part of the Topical Collection on *Image & Signal Processing*

✉ Pengjiang Qian
qianpjiang@jiangnan.edu.cn

1 School of Digital Media, Jiangnan University, 1800 Lihu Avenue, Wuxi, Jiangsu 214122, People's Republic of China

2 Changshu No.1 people's hospital, Changshu, Jiangsu 215500, People's Republic of China

3 Department of Nephrology, the Affiliated Wuxi People's Hospital of Nanjing Medical University, 299 Qingyang Rd, Wuxi, Jiangsu 214023, People's Republic of China

4 Department of Radiotherapy, Affiliated Hospital, Jiangnan University, 200 Huihe Rd, Wuxi, Jiangsu 214062, People's Republic of China

however, many disadvantages remain in traditional segmentation methods. To overcome this challenge, we employed a multitask learning and clustering algorithm to extensively leverage knowledge common among image segmentation tasks on different patients.

Clustering algorithms, which are commonly recognized as unsupervised learning preprocessing methods, are widely used in image segmentation, data mining, file recovery and pattern classification [4]. With the rapid development of technology and the appearance of new demands, many multiview clustering algorithms [5–8], transfer-learning clustering algorithms [9, 10], multitask clustering algorithms [11, 12], and subspace clustering algorithms have been proposed to challenge the disadvantages that exist in classic clustering methods. Multitask clustering algorithms, which transfer knowledge across related tasks, are widely applied to improve the clustering performance on single, related tasks. While only limited information can be exploited from the cluster structure of a single dataset, for example, bone tissue is not easy to segment in MR brain images, the multitask clustering method can improve the clustering performance of each task by leveraging knowledge across related tasks.

Since MR images of different subjects are obtained by the same scanning process, much common information could be exploited among those MR image segmentation tasks. To utilize the related information and to improve the segmentation performance, a novel distributed multitask fuzzy c-means (MT-FCM) clustering algorithm, which can extract common and individual information from multitask data, is adopted to complete the MR image segmentation tasks. In general, the contributions of our research in this manuscript are summarized as follows:

1) Considering the advantages of multitask learning, the distributed MT-FCM algorithm achieves better performance both in metrics and visualization performance compared with each single MR image segmentation task.
2) The public cluster centroids representing related information of different tasks are shared, which avoids the negative effect of noise that exists in raw data instances.
3) The simple sampling strategy is applied in our distributed MT-FCM segmentation algorithm, which can reduce the clustering time consumption and facilitate the practicability of our algorithm.

The remainder of this paper is organized as follows. In Section 0, the classic fuzzy c-mean algorithm and the multitask learning strategy are briefly introduced. In Section 0, the proposed distributed multitask fuzzy c-means algorithm and the details of the MRI dataset used in the experiment are introduced. The corresponding experimental results and discussion are illustrated in Section 0. Section 0 gives the conclusion.

Related work

Fuzzy C-means clustering

JC Bezdek et al. [13–15] proposed the fuzzy c-means (FCM) clustering method to divide target data into several categories. The FCM algorithm aims to maximize the interclass separation and minimize the intraclass variance. Let $X = \{\boldsymbol{x_j} | \boldsymbol{x_j} \in R^d, j = 1, \ldots, N\}$ denote a given dataset consisting of N data instances, and d and N signify the data dimension and data capacity, respectively. Suppose C $(1 < C < N)$ potential clusters exist in this data set. The framework of the FCM algorithm can be formulated as follows:

$$\min_{U,V}\left(J_{FCM}(U,V)=\sum_{i=l}^{C}\sum_{j=1}^{N}u_{ij}^{m}\left\|x_j-v_i\right\|^2\right), s.t. 0\le u_{ij}\le 1 \ and \ \sum_{i=1}^{C}u_{ij}=1 \tag{1}$$

where is the cluster centroid matrix,; denotes the membership matrix, and each signifies the fuzzy membership of data instance to cluster centroid; and is the fuzzy index.

Using Lagrange optimization, the updated equation of membership and cluster centroid in Eq. (1) can be separated as

$$u_{ij}=\frac{1}{\sum_{k=1}^{C}\left(\frac{\|x_j-v_i\|}{\|x_j-v_k\|}\right)^{\frac{2}{m-1}}}, i=1,\ldots,C; j=1,\ldots,N \tag{2}$$

$$v_i=\frac{\sum_{j=1}^{N}u_{ij}^{m}x_j}{\sum_{j=1}^{N}u_{ij}^{m}}, i=1,\ldots,C \tag{3}$$

Multitask learning strategy

Multitask learning [16] utilizes transferring knowledge across related tasks to improve the learning performance of each task. Four types of transferring information exist in multitask learning, i.e., transferring information of raw data instances [17–19], transferring information of parameters [20], transferring knowledge of features [3] and transferring information of relational knowledge [1, 2, 21].

Raw data instances in different tasks reflect the direct information of each task, which may include some noisy information, especially in MR image data, and can lead to negative learning across tasks. Given the feature transferring strategy, which requires that each task achieves a shared feature space and that the same set of centroids are shared in all tasks, and the parameter transferring strategy, which assumes that some parameters are shared in models for related tasks, we adopt the transferring knowledge of the relational knowledge strategy to exploit information among each task.

A distributed multitask fuzzy C-means algorithm for MR brain image segmentation

As a classical data-driven space partitioning method, the FCM algorithm has attained great success in different applications in finding the fuzzy partition corresponding to the antecedents of fuzzy systems. However, the classical FCM algorithm was only developed for the traditional single-task clustering scene. It cannot be directly utilized to handle all the datasets in a multitask scene simultaneously. The commonly adopted solution is to use the FCM algorithm to independently cluster the data of different tasks. This process makes it difficult to find the common information of all the involved tasks as well as the individual information of each task by using the classical FCM algorithm. To improve the modeling performance for the multitask scene, a co-learning framework between different tasks based on the above common and individual information of different tasks is exploited. Hence, new FCM algorithms for multitask fuzzy systems modeling are proposed, and they represent very valuable work in the field. In the following subsection, the novel distributed multitask FCM algorithm is presented.

A distributed multitask fuzzy C-means algorithm

For a multitask clustering problem, given a multitask dataset containing K tasks $\{T^1, T^2, \ldots, T^K\}$, each task corresponds to a dataset with N_k data samples, denoted as $\mathbf{X}^k = \{\mathbf{x}_{i,k}, i = 1, \ldots, N_k\}$, where $\mathbf{x}_{i,k} \in R^d$.

To extract the common information and to mine the individual information from the multitask data, we redesign two new objective functions based on the FCM algorithm by introducing multitask learning mechanisms. In this paper, the objective function of multitask fuzzy c-means clustering algorithm (the MT-FCM algorithm), is proposed,. The objective function of the MT-FCM algorithm is defined as:

$$\begin{aligned}&\min_{U,V,R,O} J_{MT-FCM}\\&(U,V,R,O) = \sum_{k=1}^{K}\sum_{j=1}^{C_k}\sum_{i=1}^{N_k} u_{ij,k}^m \left\|X_{i,k}-V_{j,k}\right\|^2\\&+\lambda_a\sum_{p=1}^{P}\sum_{i=1}^{\tilde{N}} r_{ip}^m\left\|\tilde{x}_i-o_p\right\|^2-\lambda_b\sum_{k=1}^{K}\sum_{p=1}^{P}\sum_{j=1}^{C_k}\left\|V_{j,k}-o_p\right\|^2 \text{s.t.} u_{ij,k}\in[0,1], \textstyle\sum_{j=1}^{C_k}u_{ij,k}\\&=1, \textstyle\sum_{p=1}^{P} r_{ip}=1, 1\le i\le N_k, 1\le j\le C_k, 1\le k\le K, \tilde{N}=\sum_{k=1}^{K}N_k.\end{aligned} \tag{4}$$

In this objective function, $\mathbf{x}_{i,k}$ represents the ith data sample of the kth task; $\tilde{\mathbf{x}}_i$ represents the ith data sample of the dataset containing the data samples of all the tasks; $\mathbf{U}_k = \left[\mu_{ij,k}\right]_{C_k\times N_k}$ is the private fuzzy partition matrix of the kth task; $\mathbf{V}_k = \left[\mathbf{v}_{1,k}, \ldots, \mathbf{v}_{C_k,k}\right]$ is the private cluster center of the kth task; $\mathbf{R} = \left[\mathbf{r}_1, \ldots, \mathbf{r}_{\tilde{N}}\right]$ is the set of public fuzzy partition matrices for all tasks; $\mathbf{O} = [\mathbf{o}_1, \ldots, \mathbf{o}_P]$ is the set of public cluster center for all tasks; and λ_a and λ_b are two balance parameters to control the influence of different terms. The parameters $\lambda_a(\lambda_a > 0)$ and $\lambda_b(\lambda_b > 0)$can be determined by using the grid search strategy or the cross-validation strategy. In this study, we used the grid search strategy to obtain the optimized values of these two parameters.

Remark 1 From the proposed objective function of the MT-FCM algorithm, i.e., Eq. (4), we can obtain the following observations: (1) the first term actually uses the classical FCM objective function to learn the private fuzzy partition matrices and the cluster centers for different tasks independently. (2) The second term uses the FCM objective function to learn a common fuzzy partition matrix and a cluster center matrix for the data of all tasks. (3) The third term is a term to measure the difference between the private clusters of different tasks and the public clusters of all tasks. Its purpose is to make the individual information (the private cluster centers of each task) as different as possible from the common information (the public cluster centers of all tasks). By integrating the above three terms in Eq. (4), a novel multitask fuzzy c-means clustering algorithm is proposed.

Next, we can solve Eq. (4) to obtain the optimal solution for multitask FCM clustering. Accordingly, the Lagrangian function of Eq. (4) can be expressed as:

$$\begin{aligned}J(\mathrm{U,R,V,O}) = &\sum_{k=1}^{K}\sum_{j=1}^{C_k}\sum_{i=1}^{N_k} u_{ij,k}^m\left\|\mathrm{x}_{i,k}-\mathrm{v}_{j,k}\right\|^2+\lambda_a\sum_{p=1}^{P}\sum_{i=1}^{\tilde{N}} r_{ip}^m\left\|\tilde{\mathrm{x}}_i-\mathrm{o}_p\right\|^2\\&-\lambda_b\sum_{k=1}^{K}\sum_{p=1}^{P}\sum_{j=1}^{C_k}\left\|\mathrm{v}_{j,k}-\mathrm{o}_p\right\|^2+\sum_{k=1}^{K}\sum_{i=1}^{N_k}\alpha_{i,k}\left(1-\textstyle\sum_{j=1}^{C}u_{ij,k}\right)\\&+\sum_{i=1}^{\tilde{N}}\beta_i\left(1-\textstyle\sum_{p=1}^{P}r_{ip}\right)\end{aligned} \tag{5}$$

Then, we can derive the following update equations as the learning rules for the solution variables of our multitask FCM clustering:

$$u_{ij,k} = 1\Big/\sum_{l=1}^{C}\left(\left\|\mathrm{x}_{i,k}-\mathrm{v}_{j,k}\right\|^2\Big/\left\|\mathrm{x}_{i,k}-\mathrm{v}_{l,k}\right\|^2\right)^{\frac{1}{m-1}} \tag{6}$$

$$\mathrm{V}_{j,k} = \left(\sum_{i=1}^{N_k}u_{ij,k}^m\mathrm{x}_{i,k}-\lambda_b\sum_{p=1}^{P}\mathrm{o}_p\right)\Big/\left(\sum_{i=1}^{N_k}u_{ij,k}^m-\lambda_b P\right) \tag{7}$$

$$r_{ip} = 1\Big/\sum_{l=1}^{P}\left(\frac{\left\|\tilde{\mathrm{x}}_i-\mathrm{o}_p\right\|^2}{\left\|\tilde{\mathrm{x}}_i-\mathrm{o}_l\right\|^2}\right)^{\frac{1}{m-1}} \tag{8}$$

$$\mathrm{o}_p = \left(\lambda_a\sum_{i=1}^{\tilde{N}}r_{ip}^m\tilde{\mathrm{x}}_i-\lambda_b\sum_{k=1}^{K}\sum_{j=1}^{C_k}\mathrm{v}_{j,k}\right)\Big/\left(\lambda_a\sum_{i=1}^{\tilde{N}}r_{ip}^m-\lambda_b\sum_{k=1}^{K}C_k\right) \tag{9}$$

According to the update equations above, the algorithm of the distributed MT-FCM algorithm can be summarized as follows. The workflow of the distributed MT-FCM algorithm is shown in Fig. 1.

clustering algorithm. In the near future, we will try to address the more challenging application of multitask clustering where the numbers of clusters in different tasks are assumed to be unknown.

Algorithm: MT-FCM	
Step 1	Given K tasks, the number of private clusters C_k $(2 \le C_k < N_k)$ for N_k sample points in the kth task, the number of public clusters $P(2 \le P < \tilde{N})$ for $\tilde{N}$ sample points of all tasks, the convergence threshold ε, the fuzzy index m, the balance parameters $\lambda_a(\lambda_a > 0)$, $\lambda_b(\lambda_b > 0)$ and the maximum number of iterations T, initialize the private cluster center $\mathbf{v}_{j,k}$ for each task and the public cluster center $\mathbf{o}_p$ for all tasks; Set the initial value of iteration number $s = 1$.
Step 2	Update the private fuzzy membership $\mu_{ij,k}^{(s+1)}$ using (6) for each task.
Step 3	Update the private clustering centers $\mathbf{v}_{j,k}^{(s+1)}$ using (7) for each task.
Step 4	Update the public fuzzy membership $r_{ip}^{(s+1)}$ using (8).
Step 5	Update the public cluster centers $\mathbf{o}_p^{(s+1)}$ using (9).
Step 6	If $\left\|J^{(s+1)} - J^{(s)}\right\| < \varepsilon$ or if the number of iterations $l > T$, then terminate; otherwise, let $l = l + 1$ and go to step 2.

Remark 2 Although the abovementioned MT-FCM clustering algorithm is a promising method to solve the problem of multitask clustering and to extract the common information of all tasks and the individual information for each task, there are still a few weaknesses as follows: i) The objective function essentially contains two parts, i.e., the first and the second terms, to realize the clustering. One part completes the local clustering for each task, and the other part obtains the global clustering for all tasks. Both parts work on the original data $\mathbf{x}$ in different tasks and do not use any advanced clustering information; ii) Although the third term is effectively used to control for the differences between the private clusters of different tasks and the public clusters of all tasks, it is not a trivial matter to control it in practical applications; iii) Two balance parameters, λ_a and λ_b, must be adjusted, which leads to a high computational cost to optimize these parameters; iv) The computational complexity of the proposed MT-FCM algorithm is $O\left(TK\sum_{k=1}^{K}(N_kC_k) + TK\sum_{k=1}^{K}(C_k) + T\tilde{N}P + TP\right)$, where T is the maximum number of iterations. In theory, the speed of the proposed multitask fuzzy c-means clustering algorithm is slow compared to that of the corresponding non multitask clustering algorithms; v) The number of clusters for different tasks is assumed to be known for our proposed multitask

UTE-mDixon PET/MR brain images

The ultrashort echo time (UTE) and the modified Dixon PER/MR [22–26] brain image datasets in our work consist of three different sequences, i.e., Dixon (fat only), Dixon (water only), and $R2^*$, from six patients. Each MRI dataset was composed of 256 image slices with a resolution of 256×256 pixels. Fig. 2 images show the original images with Dixon-fat, Dixon-water, and $R2^*$ of one patient, which are utilized as the inputs in the MT-FCM clustering algorithm.

Experimental results

Setup

In a medical image segmentation process, the data capacity can be up to several million data instances. To promote the feasibility of the algorithm, a simple sample strategy is applied in the process of the clustering algorithm, and the labels of the leftover data instances are achieved by a k-nearest neighbor strategy. In addition, the sampling strategy is designed to guarantee consistency in each algorithm to ensure the fairness in the quality of the random data. All metrics are reported after

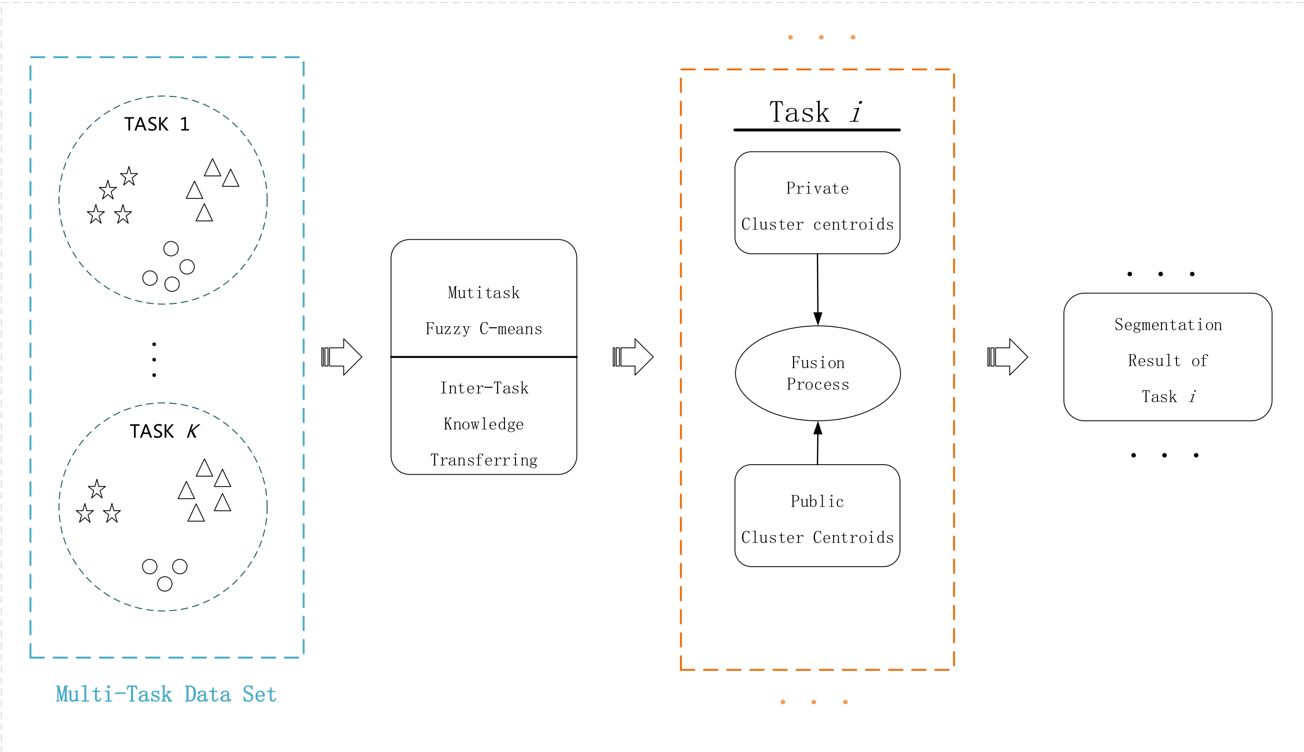

Fig. 1 Workflow of the distributed MT-FCM algorithm

ten runs of each method under each parameter set to measure the robustness of the sampling strategy and the algorithm's performance.

To illustrate the effectiveness of our proposed MT-FCM MR brain image segmentation method, the classic single task FCM (ST-FCM) algorithm has been adopted as a comparison. The parameter settings of each algorithm are shown as follows: For the ST-FCM algorithm, the fuzzy index is set within the set {1.1: 0.1: 2.5}. For our MT-FCM algorithm, the regularization parameters λ_a and λ_b are both set within the set $\{10^{-6},10^{-5},\ldots,10^{5},10^{6}\}$. In our experiment, all the parameters can be determined by using a grid search strategy. All data were normalized to the interval [0, 1] before they were used in the experiments.

While it is impossible to obtain a precise ground segmentation reference of each MR image, we generate a pseudo-CT image [26, 27] for each MR image by assigning the HU value based on the partition results of each algorithm to each segmented tissue. To illustrate the segmentation performance, we compared the pseudo-CT with the real CT corresponding to each MR brain image. Three validity metrics, such as the root mean square error (RMSE), the mean absolute prediction deviation (MAPD), and R [26], were used for the performance comparisons. Values of RMSE and MAPD close to 0 and values of R close to 1 indicate better performance. All experiments were conducted using a PC with an Intel Core i5–4590 3.30 GHz CPU, 12 GB of RAM, Microsoft Windows 10 (64 bit), and MATLAB R2016a (64 bit).

Fig. 2 UTE-mDixon MR images

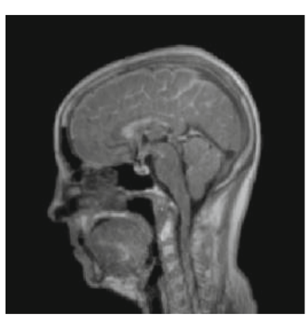

(a) Dixon (fat only)

(b) Dixon (water only)

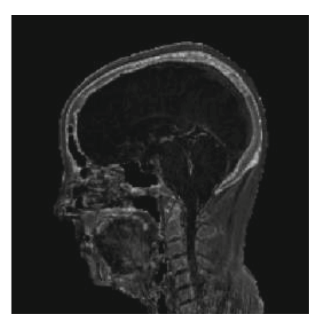

(c) *R2**

Table 1 Performance comparison of the ST-FCM algorithm and the MT-FCM algorithm on the MR brain image segmentation tasks

Dataset		RMSE		MAPD		R		Time/s		
		ST-FCM	MT-FCM	ST-FCM	MT-FCM	ST-FCM	MT-FCM	ST-FCM		MT-FCM
								Single Task	Task Group	
Patient 1	mean	201.1027	**189.6785**	110.9121	**100.3061**	0.8539	**0.8641**	5.6195	18.4832	25.5543 (±0.0253)
	std	20.9535	2.4836	16.0934	0.8042	0.0219	0.0036	0.0550		
Patient 2	mean	260.9469	**240.4876**	141.3902	**128.0083**	0.7293	**0.7763**	6.9606		
	std	37.5130	0.5351	20.2085	0.4361	0.0786	0.0018	0.0641		
Patient 3	mean	205.2662	**202.2946**	119.8958	**110.7344**	0.8244	**0.8368**	5.9031		
	std	26.9673	12.0157	15.9854	8.2126	0.0429	0.0038	0.1199		
Patient 4	mean	232.9017	**220.0795**	137.7546	**128.4882**	0.8357	**0.8548**	6.2912	19.2462	21.2721 (±0.2948)
	std	25.3690	8.9339	17.3646	5.4113	0.0234	0.0035	0.3383		
Patient 5	mean	238.9699	**239.7784**	123.9699	**124.6259**	0.7974	**0.8099**	6.8111		
	std	12.3890	0.9607	11.4116	0.8624	0.0193	0.0010	0.2254		
Patient 6	mean	220.5533	**205.0513**	131.7083	**115.4866**	0.7766	**0.7974**	6.1439		
	std	11.6982	18.8061	4.2225	7.8481	0.0184	0.0422	0.1489		
Patient 7	mean	194.4721	**192.0314**	109.5634	**105.2172**	0.8498	**0.8524**	5.6243	17.8680	20.1923 (±0.2701)
	std	15.9285	0.8189	11.9622	0.5263	0.0179	0.0013	0.0865		
Patient 8	mean	249.3192	**238.7492**	127.1932	**120.3547**	0.6956	**0.7549**	5.9084		
	std	39.3816	4.4959	23.2347	3.7403	0.0971	0.0001	0.2253		
Patient 9	mean	210.4900	**194.4711**	120.2374	**111.2510**	0.8767	**0.8916**	6.3353		
	std	17.5452	1.4472	12.9469	1.2883	0.0149	0.0010	0.1953		

Bolds entries denote the best results obtained by the adopted methods on the given tasks

Results and discussion

There were nine patients in the dataset. Table 1 shows the experimental results of the comparison between the ST-FCM algorithm and the MT-FCM algorithm, including the means and standard deviations of the RMSE, MAPD and R values. Table 2 illustrates the best parameter settings of the proposed two methods for all datasets.

From the results of Table 1, it is obvious that the proposed MT-FCM algorithm achieves relatively high metrics for transferring knowledge of different tasks. However, during the MT-FCM clustering process, more time is required to exploit the knowledge from each task, such as the public fuzzy partition matrix and the public cluster centers; the amount of time consumed by the MT-FCM algorithm is slightly higher than the sum of the amounts of time consumed by each task by the ST-FCM algorithm. Based on the partition results, a fixed linear attenuation coefficient (LAC) is assigned to each corresponding tissue type, and the pseudo-CT images are shown in Fig. 3.

Table 2 The best parameter settings for the proposed two methods for all datasets

Dataset	Parameters		
	ST-FCM	MT-FCM	
	Fuzzy index m	regularization parameter λ_a	regularization parameter λ_b
Patient 1	1.5	1.00E-04	0.01
Patient 2	1.2	0.001	0.1
Patient 3	1.7	0.1	100
Patient 4	1.6	10,000	1.00E-04
Patient 5	1.6	0.01	0.01
Patient 6	1.9	0.01	100
Patient 7	1.5	1	100
Patient 8	1.7	0.001	1
Patient 9	1.3	10	10

Table 1 and Fig. 3 illustrate the segmentation performance of the single-task FCM and multitask FCM algorithms, and the following can be analyzed:

1) Compared with the classic single-task FCM algorithm, the proposed multitask FCM algorithm demonstrates better segmentation performance from the metric value. In addition, the lower standard deviation of the three metrics indicates that the MT-FCM algorithm is more robust based on the parameter settings.
2) From the visualization results of the pseudo-CT images, the MT-FCM algorithm could distinguish different tissue types, such as bone, soft tissue and air, more precisely than the classic FCM algorithm.
3) Considering the advantage of knowledge among related MR segmentation tasks, the MT-FCM algorithm could partition different tissue types more precisely and avoid

Fig. 3 Pseudo-CT images from the ST-FCM and MT-FCM algorithms for Patient 1 and Patient 2

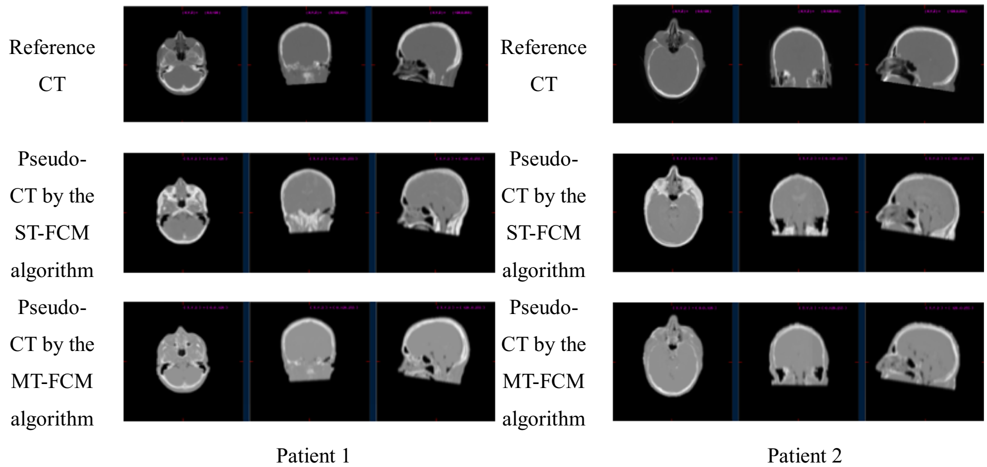

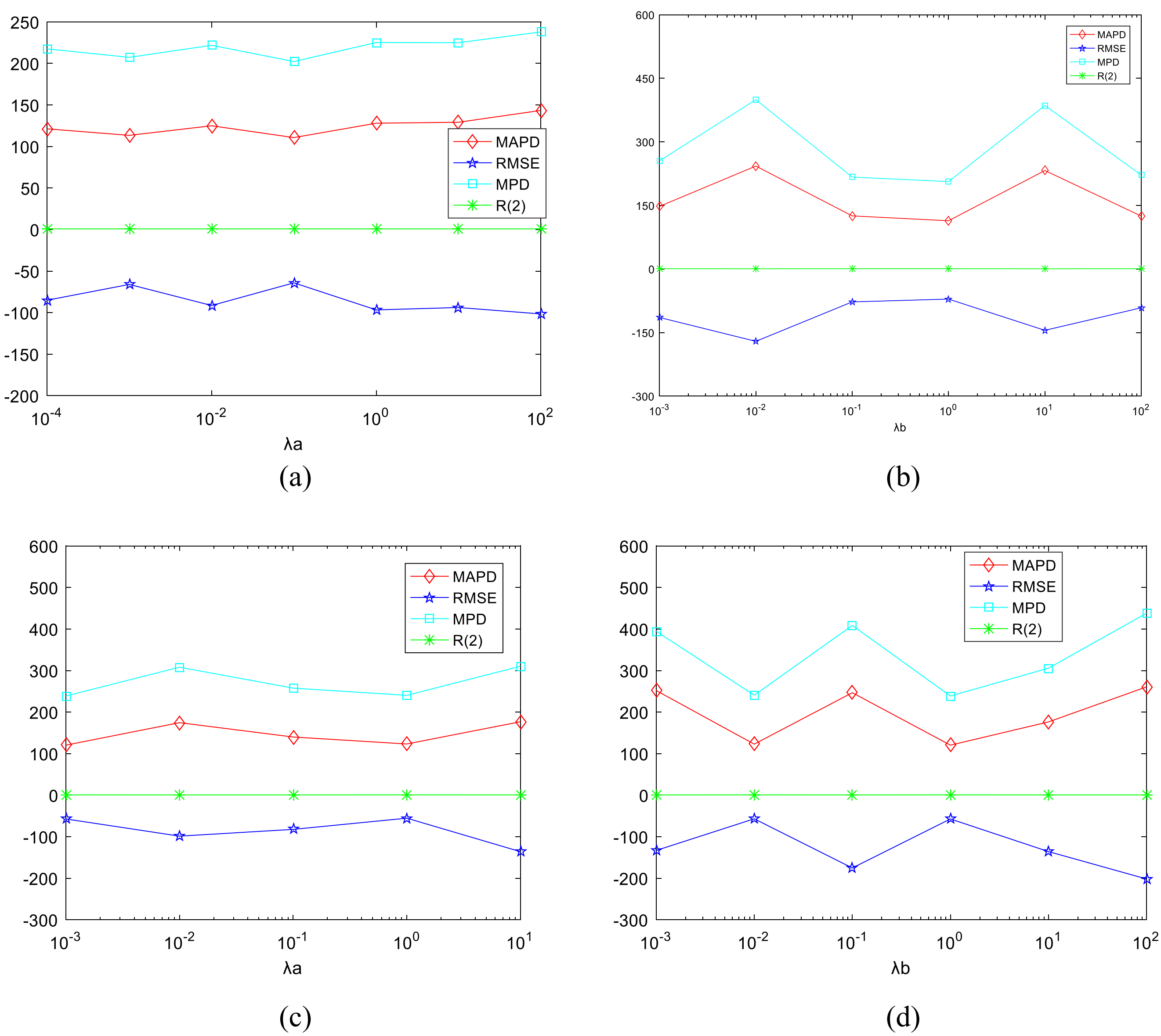

Fig. 4 Parameter analysis of KTOFC-MRAC with respect to parameters β and γ. (a) λ_a VS Patient 3; (b) λ_b VS patient 3; (c) λ_a VS patient 8; (d) λ_b VS patient 8

some of the negative effects caused by noisy data in a single dataset. Therefore, the pseudo-CT images generated by the MT-FCM algorithm demonstrate a clearer and more complete picture.

Sensitivity analysis

To completely demonstrate the reliability of our proposed method, we have also assessed the parameter robustness of our proposed MT-FCM method with respect to the core parameters, i.e., the regularization coefficients λ_a and λ_b involved. Figs. 4(a) and 4(c) illustrate the sensitivity of parameter λ_a with respect to the two patients' results, which indicate that the proposed MT-FCM method is relatively stable with respect to this parameter. Figs. 4(b) and 4(d) show that our method is also not very sensitive to the regularization parameter λ_b.

From the above, we know that our proposed MT-FCM method is relatively stable when the core parameters are located within proper ranges.

Conclusions

In this paper, a multitask fuzzy c-means clustering algorithm is adopted for multiple MR image sequence segmentation. Our proposed method can take advantage of exploiting common knowledge among related tasks to improve the segmentation performance of each task. According to the segmentation results, as illustrated by three metrics and the pseudo-CT images, the proposed MT-FCM algorithm achieves competitive performance over the classic single-task FCM algorithm. In general, the contribution of this paper is as follows: 1) The multitask clustering algorithm can effectively utilize the information common among related tasks to improve performance in the MR brain image performance. 2) The MT-FCM algorithm can take advantage of extracted knowledge rather than raw data in related tasks to improve the clustering performance and avoid the negative effects caused by noisy raw data in MR images. 3) The simple sampling strategy is applied in our MT-FCM segmentation algorithm, which could reduce the clustering time consumption and facilitate the practicability of our algorithm. However, our proposed method requires more runtime to adjust the regularization parameter than the classic FCM algorithm, which may become a hamper in clinical application. In our future work, we will focus on optimizing the parameter settings and applying our method to more challenging MR images, such as those of the abdomen.

Acknowledgements This work was supported in part by the National Natural Science Foundation of China under Grants 61702225 and 61772241, by the Natural Science Foundation of Jiangsu Province under Grant BK20160187, by the 2018 Six Talent Peaks Project of Jiangsu Province under Grant XYDXX-127, by the Science and technology demonstration project of social development of Wuxi under Grant WX18IVJN002,by the Youth Foundation of the Commission of Health and Family Planning of Wuxi under Grant Q201654, and by the Jiangsu Committee of Health under Grant H2018071.

Compliance with ethical standards

Conflict of interest The authors declare that there is no conflict of interests of this paper. This article does not contain any studies with human participants or animals performed by any of the authors. Informed consent was obtained from all individual participants included in the study.

References

1. Jiang, Y., Deng, Z., Chung, F. L. et al., Multi-task TSK fuzzy system modeling using inter-task correlation information. Information Sciences 298:512–533, 2015.
2. Mihalkova L, Mooney R J. Transfer learning from minimal target data by mapping across relational domains. International Jont conference on Artifical intelligence. Morgan Kaufmann publishers Inc. 2009.
3. Argyriou, A., Evgeniou, T., and Pontil, M., Multi-task feature Learning. Advances in Neural Information Processing Systems 19:41–48, 2006.
4. Sato-Ilic, M., Fuzzy variable selection with degree of classification based on dissimilarity between distributions of variables. International Journal of Intelligent Technology and Applied Statistics 1:1–18, 2008.
5. Jiang, Y., Deng, Z., Chung, F. L. et al., Realizing two-view TSK fuzzy classification system by using collaborative Learning. IEEE Transactions on Systems Man & Cybernetics Systems 47:145–160, 2017.
6. Yamanishi Y, Vert J P, Kanehisa M. Protein network inference from multiple genomic data: A supervised approach. Oxford University Press, 2004.
7. Cleuziou G, Exbrayat M, Martin L, et al. CoFKM: A centralized method for multiple-view clustering, Ninth IEEE International Conference on Data Mining. IEEE Computer Society, 2009.
8. Qian, P., Zhou, J., Jiang, Y. et al., Multi-view maximum entropy clustering by jointly leveraging inter-view collaborations and intra-view-weighted attributes. IEEE Access 6:28594–28610, 2018.
9. Deng, Z., Jiang, Y., Chung, F. L. et al., Transfer prototype-based fuzzy clustering. IEEE Transactions on Fuzzy Systems 24:1210–1232, 2014.
10. Qian, P., Jiang, Y., Deng, Z. et al., Cluster prototypes and fuzzy memberships jointly leveraged cross-domain maximum entropy clustering. IEEE Transactions on Cybernetics 46:181, 2016.
11. Caruana, R., Multitask Learning. Machine Learning 28:41–75, 1997.
12. Jiang, Y., Chung, F. L., Ishibuchi, H. et al., Multitask TSK fuzzy system modeling by mining Intertask common hidden structure. IEEE Transactions on Cybernetics 45:534–547, 2017.
13. Bezdek, J. C., Ehrlich, R., and Full, W., FCM: The fuzzy c-means clustering algorithm[J]. Computers & Geosciences 10:191–203, 1984.
14. Qian, P., Zhao, K., Jiang, Y. et al., Knowledge-leveraged transfer fuzzy C -means for texture image segmentation with self-adaptive cluster prototype matching. Knowledge-Based Systems 130, 2017.
15. Qian, P., Jiang, Y., Deng, Z. et al., Cluster prototypes and fuzzy memberships jointly leveraged cross-domain maximum entropy clustering. IEEE Transactions on Cybernetics 46:181, 2016.

16. Pan, S. J., and Yang, Q., A survey on transfer Learning. IEEE Transactions on Knowledge & Data Engineering 22:1345–1359, 2010.
17. Zadrozny B. Learning and evaluating classifiers under sample selection bias, 2004.
18. Dai W, Xue G R, Yang Q, et al. Transferring Naive Bayes Classifiers for Text Classification, National Conference on Artificial Intelligence. AAAI Press, 2007.
19. Dinuzzo, F., Learning output kernels for multi-task problems. Neurocomputing 118:119–126, 2013.
20. Zheng, H., Geng, X., Tao, D. et al., A multi-task model for simultaneous face identification and facial expression recognition. Neurocomputing 171:515–523, 2016.
21. Jiang, Y., Deng, Z., Choi, K. S. et al., A novel multi-task TSK fuzzy classifier and its enhanced version for labeling-risk-aware multi-task classification. Information Sciences 357:39–60, 2016.
22. Hooijmans, M. T., Dzyubachyk, O., Nehrke, K. et al., Fast multistation water/fat imaging at 3T using DREAM-based RF shimming. Journal of Magnetic Resonance Imaging 42:217–223, 2015.
23. Eggers, H., Brendel, B., Duijndam, A. et al., Dual-echo Dixon imaging with flexible choice of echo times. Magnetic Resonance in Medicine 65:96–107, 2011.
24. Zaidi, H., Ojha, N., Morich, M. et al., Design and performance evaluation of a whole-body ingenuity TF PET-MRI system. Physics in Medicine & Biology 56:3091–3106, 2011.
25. Kalemis, A., Delattre, B. M., and Heinzer, S., Sequential whole-body PET/MR scanner: Concept, clinical use, and optimisation after two years in the clinic. The manufacturer's perspective. Magma 26:5–23, 2013.
26. Su, K. H., Hu, L., Stehning, C. et al., Generation of brain pseudo-CTs using an undersampled, single-acquisition UTE-mDixon pulse sequence and unsupervised clustering. Medical Physics 42:4974–4986, 2015.
27. Johansson, A., Karlsson, M., Yu, J. et al., Voxel-wise uncertainty in CT substitute derived from MRI. Medical Physics 39:3283–3290, 2012.